Rigid rod polymers with flexible side chains

Synthesis, structure and phase behaviour of poly(3-*n*-alkyl-4-oxybenzoate)s*

R. Stern, M. Ballauff†, G. Lieser and G. Wegner
Max-Planck-Institut für Polymerforschung, Postfach 3148, 65 Mainz, Germany
(Received 26 February 1990; revised 31 July 1990; accepted 31 July 1990)

The synthesis of poly(3-*n*-alkyl-4-oxybenzoate)s (PAOB-*n*) with $n=3$–18 is reported. The sufficient solubility of these comb-like polymers with stiff-chain backbones allows the determination of the Kuhn length (100–200 Å). The unit cells could be determined for PAOB-*n* with $n=3$ and 5. All PAOB-*n* form thermotropic mesophases. For $n=3$ a nematic phase is found. For $n=5$ there is a transition from a smectic-like, layered mesophase to a nematic mesophase. PAOB-*n* with $n \geqslant 6$ solely form layered mesophases. Except for $n=3$, all PAOB-*n* exhibit a transition to the isotropic state. The transition temperature is lowered monotomically with increasing *n*.

(Keywords: rigid rod polymer; synthesis; phase behaviour)

INTRODUCTION

Rigid rod polymers usually exhibit very low solubility and melting points far above the temperatures of thermal decomposition. In a number of recent publications it has been shown that flexible side chains appended to the rigid backbones lower the melting point and increase the solubility in a systematic fashion[1]. Most of the fully aromatic systems studied so far are composed of rather symmetric repeating units, i.e. the different conformers of these polymers exhibit nearly the same shape. Asymmetric monomers, on the other hand, should cause a further disturbance of crystallization because of the vast number of shapes generated by different conformers. In this work we present a comprehensive study of the poly(3-*n*-alkyl-4-oxybenzoate)s(PAOB-*n*)

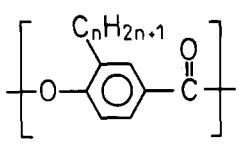

as an example of a comb-like polymer composed of asymmetric repeating units. The number of carbon atoms *n* in the side chains is varied between 3 and 18, thus PAOB-12 is poly(3-dodecyl-4-oxybenzoate). The choice of poly(4-oxybenzoate) as the stiff backbone derives from the fact that this polymer has already been the subject of a number of exhaustive studies[2–7]. Hence the influence of the side chains on the structure can be assessed in detail by comparing the results found here with the data obtained on the unsubstituted poly(4-oxybenzoate). Together with a previous investigation[8] of defined oligomers of PAOB-3 the present study aims at a full understanding of the structure and the phase behaviour of these comb-like polyesters.

The synthesis of the monomers, the 3-*n*-alkyl-4-hydroxybenzoic acids (**1**–*n*), proceeds along the following lines: the monomer bearing the propyl substituent (**1**–3, $n=3$) is easily available from the 3-allyl-4-hydroxybenzoic acid[9] through catalytic hydrogenation at atmospheric pressure. The monomers bearing longer *n*-alkyl chains (**1**–5 to **1**–18) are obtained through a Fries rearrangement[10] of the respective O-acylated 4-hydroxybenzoic acids (**2**-*n*) and subsequent Clemmensen reduction of the ketones **3**–*n* (*Scheme 1*). The polycondensation of the monomers **1**–*n* is performed by heating the monomer with an excess of acetic anhydride (cf. ref. 3).

EXPERIMENTAL

Materials

All chemicals were purchased from Merck or Fluka. They were used without further purification unless otherwise stated. All solvents used were of p. a. quality; 1,1,2,2-tetrachloroethane, phenol and *o*-dichlorobenzene employed as solvents for viscosity measurements were distilled prior to use.

Synthesis of monomers

1,3-Propyl-4-hydroxybenzoic acid (*1–3*). The 3-allyl-4-hydroxybenzoic acid was synthesized through Claisen rearrangement of ethyl-4-allyloxybenzoate which was prepared from ethyl-4-hydroxybenzoate[9]. Hydrogenation using palladium on charcoal as catalyst and subsequent saponification in 30% aqueous sodium hydroxide solution led to 3-propyl-4-hydroxybenzoic acid. The monomer

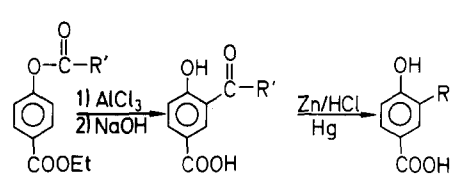

Scheme 1

* Part of the *PhD Thesis* of R. Stern
† To whom correspondence should be addressed. Present address: Polymer-Institut der Universität Karlsruhe, Kaiserstr. 12, 7500 Karlsruhe, Germany

0032-3861/91/112096-10

Table 1 Melting points and elemental analyses of the 3-*n*-alkyl-4-hydroxybenzoic acids (**1**–*n*)

n	Melting point (°C)	Calc. C (%)	Calc. H (%)	Found C (%)	Found H (%)
3	115–118	66.64	6.73	66.58	6.76
5	126–127	69.20	7.76	69.39	7.75
6	100–101	70.23	8.18	70.11	8.14
10	103–104	73.33	9.43	73.46	9.26
12	98–99	74.45	9.89	74.38	9.77
14	101–102	75.39	10.26	75.53	10.14
16	100–102	76.18	10.58	76.31	10.36
18	100–101	76.86	10.86	76.91	10.77

^{1}H n.m.r. (acetone): $\delta = 0.89$ (t, CH_2CH_3), 1.2–1.7 (m, $-(CH_2)_n-$), 2.69 (t, Ar–CH_2–), 6.93, 7.72 (d, Ar–H), 7.82 (s, Ar–H)

Table 2 Melting points and elemental analyses of the 3-(*n*-alkyl-2-one)-4-hydroxybenzoic acids (**3**–*n*)

n	Melting point (°C)	Elemental analysis: Calc. C (%)	Calc. H (%)	Found C (%)	Found H (%)
6	191–193	66.08	6.84	66.13	6.71
10	185–187	69.82	8.29	70.00	8.13
12	179–180	71.20	8.82	71.32	8.70
14	174–176	72.36	9.27	72.22	9.13
16	173–175	73.35	9.66	73.57	9.53
18	168–170	74.20	9.98	73.07	9.90

^{1}H n.m.r. (trifluoroacetic acid): $\delta = 0.95$ (t, CH_2CH_3), 1.2–2.2 (m, $-(CH_2)_n-$), 3.24 (t, $COCH_2CH_2$), 7.18 and 8.34 (d, Ar–H), 8.81 (s, Ar–H)

1–3 was purified from H_2O and dried carefully prior to use. The overall yield of the four-step reaction was 45%. The melting point and the elemental analysis of **1**–3 is given in *Table 1*.

Synthesis of monomers 1–5 to 1–18. The ethyl-4-alkanoyloxybenzaotes **2**–5 to **2**–18 were prepared by reacting ethyl-4-hydroxybenzoate with an excess of the respective acid chloride according to the standard procedures given in the literature[11]. The Fries rearrangement of **2**–*n* was achieved in the following way (cf. ref. 10): 0.3 mol of **2**–*n* was dissolved in 500 ml CS_2 and 1.2 mol $AlCl_3$ were added in small portions leading to a slightly exothermic reaction and evolution of HCl. After the last addition the mixture was refluxed for 3 h. Then the solvent was distilled off and the remainder heated to 140–160°C followed by evolution of HCl and strong foaming. After 2 h and cooling to room temperature 800 ml H_2O were added and subsequently 160 g NaOH with caution. The mixture dissolved upon heating to 110–120°C and the resulting ketone **3**–*n* could be isolated by acidification with 400 ml concentrated HCl. Purification was achieved through recrystallization from ethanol, toluene or chloroform (yields 40–45%). *Table 2* shows the melting points and the elemental analyses of **3**–5 to **3**–18.

The Clemmensen reduction was carried out in the usual way following references 10 and 11: 0.1 mol **2**–*n* was refluxed for 24 h in 350 ml of a mixture of H_2O/ethanol/HCl (1:1:2) with zinc amalgam prepared from 200 g zinc powder[11]. During this time 10 ml of concentrated HCl were added several times. The resulting **1**–*n* was isolated from the cold mixture by extraction with diethyl ether. Analysis by ^{1}H nuclear magnetic resonance (n.m.r.) spectroscopy demonstrated that the raw materials still contained a side product having a double bond in the α position of the alkyl side chain. For further purification 20 g of the raw material were dissolved in 300 ml ethanol and hydrogenated after addition of 0.5 g palladium on charcoal (10%) at 50°C for 24–30 h. Then the catalyst was filtered off and the monomers **1**–*n* were recrystallized three times from CH_3OH/H_2O or CH_3OH (yields 50–75%).

Polymerization (cf. ref. 3)

For the polymerization reaction, 1.5–3.0 g of **1**–*n* were added to 1.2 equivalents of acetic anhydride and refluxed under an atmosphere of argon at 180°C for 30 min. Then the condenser was taken off and the acetic acid removed by a slow stream of argon. While raising the temperature to 260°C the evolution of acetic acid started again at ~245°C. By variation of the reaction time from 45 min to 7 h polymers with different molecular weights could be obtained (*Table 3*). Purification of PAOB-3 was carried out by refluxing the polymer with acetone; polyesters with longer side chains were dissolved in hot chloroform and precipitated from methanol. All polymers reported in this investigation gave satisfactory elemental analyses when taking into account the measured molecular weights and the respective end groups.

Determination of molecular weight through end group analysis

According to Kricheldorf and Schwarz[3], 20–30 mg of the polyester PAOB-*n*, ~200 mg 40% NaOD in D_2O and 500 mg CD_3OD were weighed carefully in a n.m.r.

Table 3 Characterization of the PAOB-*n*

Polymer	Reaction time (min) 180°C/260°C	*DP*[a]	M_n[a]	$[\eta]$ (dl g^{-1})
PAOB-3,1	30/45	16	2650	
PAOB-3,2	30/60	22	3600	0.310[b]
PAOB-3,3	30/160	39	6350	0.490[b]
PAOB-3,4	30/240	123	20000	1.620[b]
PAOB-3,5[d]	30/240	74	12100	0.860[b]
PAOB-5,1	30/240	23	4450	
PAOB-5,2	30/360	40	7650	
PAOB-6,1	30/240	16	3350	
PAOB-6,2	30/360	37	7600	
PAOB-10,1	30/240	17	4500	
PAOB-10,2	30/360	41	10750	
PAOB-12,1	30/150	13	3800	
PAOB-12,2	30/300	84	24300	
PAOB-14,1	30/240	20	6400	
PAOB-14,2	60/240	27	8600	
PAOB-16,1	30/60	8	2950	0.096[c]
PAOB-16,2	30/120	16	5650	0.180[c]
PAOB-16,3	30/180	22	7550	0.290[c]
PAOB-16,4	30/240	23	7800	0.350[c]
PAOB-16,5	30/360	30	10400	0.485[c]
PAOB-16,6	30/420	40	13900	
PAOB-18	60/180	35	13100	

[a] Determined by ^{1}H n.m.r. end-group analysis
[b] Measured in phenol/*o*-dichlorobenzene (1:1) at 50°C
[c] Measured in tetrachloroethane/*o*-dichlorobenzene (1:1) at 50°C
[d] Polymerized with addition of 5 mol% 4-methoxyl-3-propylbenzoic acid

tube and heated to 50–60°C. The solution obtained was analysed by 300 MHz or 400 MHz ^{1}H n.m.r. spectroscopy to yield the amount of end groups quantitatively (see below).

Methods

^{1}H n.m.r. spectra were recorded with 80 MHz continuous wave, 300 MHz Fourier transform (*FT*) and 400 MHz *FT* spectrometers (Bruker AW 80, AC 300 and WM 400). Vapour pressure osmometry (v.p.o.) was done at 50°C using toluene as a solvent (Wescan 232 A, Corona). The concentration of the polymer was 2–10 g l^{-1}. For polarizing microscopy a Zeiss Fotomikroskop III equipped with a Leitz hot stage was used. Differential scanning calorimetry (d.s.c.) was done with a Perkin–Elmer DSC-7 calibrated with indium and tin. Thermogravimetric data were obtained by means of a TG 50 of Mettler under an atmosphere of oxygen or nitrogen employing a heating rate of 10 K min^{-1}. The intrinsic viscosity of the polyesters was determined using an Ubbelohde capillary viscosimeter. All data are mean values of at least four measurements corrected[13] according to Hagenbach. High performance liquid chromatography (h.p.l.c.) was carried out on Li Chrosorb RP 18 or Li Chrosorb diol columns (Knauer) using a mixture of diethyl acetate and n-heptane (1:1) with ultraviolet (u.v.) detection at $\lambda = 254$ nm. For gel permeation chromatography (g.p.c.) 10 μm Styragel columns (10^5, 10^3 and 10^2, Polymer Laboratories) with tetrahydrofuran (1 ml min^{-1}) as the mobile phase (u.v. detection at $\lambda = 254$ nm) were used. Wide-angle X-ray analysis (WAXS) was performed using Ni-filtered CuKα radiation in reflection mode on a Siemens D 500 diffractometer equipped with a hot stage. All diffractograms are uncorrected. Electron diffraction was done using a Philips EM 300 calibrated with thallium chloride. The density of polymer films and fibres was determined in a density gradient set up from mixtures of H_2O and $Ca(NO_3)_2$ at room temperature.

RESULTS AND DISCUSSION

All polymers investigated were synthesized by the acetoxy method[3], i.e. by reaction of the unsubstituted hydroxybenzoic acid with acetic anhydride. Since the maximum temperature applied in the course of the polycondensation did not exceed 260°C, no side products as discussed by Economy and co-workers[2] have been observed. The satisfactory degrees of polymerization achieved and the absence of any by-products to be detected in the analysis of the saponificated polyesters are furthermore indicative of the absence of side reactions. Special care has been taken to remove the evolving acetic acid as well as excess acetic anhydride by a slow stream of argon. During the reaction small amounts of a solid material sublimed out of the mixture. Analysis by infra-red (i.r.) and n.m.r. spectroscopy unambiguously demonstrated this substance to be identical with the acetylated monomer. In the case of short side chains ($n = 3$, 5, 6) the melt turned turbid after 40–120 min indicating the formation of a mesophase. For monomers having longer side chains the resulting melt became increasingly viscous during polycondensation but only turned turbid when cooled to temperatures below 200°C. As is obvious from *Table 3* the degree of polymerization (*DP*) can be adjusted by the length of the reaction time. The present data indicate that even higher molecular weights could be obtained if desired. However, raising the *DP* beyond the values given here resulted in difficulties when determining the molecular weight by end-group analysis (see below).

In contrast to the unsubstituted poly(4-oxybenzoate)[3] the PAOB-3 already exhibits sufficient solubility in mixtures like *o*-dichlorobenzene with tetrachloroethane or phenol. Polyesters bearing longer side chains may be dissolved in toluene or chloroform. Therefore purification can be achieved through dissolution in these solvents and reprecipitation into methanol. This finding is in accordance with observations on a number of other rigid rod polymers being similarly substituted by flexible side chains[1]. It indicates that the side chains act as a 'bound solvent'. However, investigations of solutions of PAOB-16 in solvents like toluene lead to the conclusion that these polyesters still have a strong tendency for association in solution. This fact may be also inferred from the formation of gels by these solutions at room temperature. Mixtures of strong polar solvents like *o*-dichlorobenzene and tetrachloroethane prevent the formation of such gels if the concentration is not too high. Up to now attempts to determine the molecular weight and the radius of gyration by light scattering have failed because of either strong association or small refractive index increment. Thus the *DP* of the polymers had to be determined by ^{1}H n.m.r. end-group analysis according to Kricheldorf and Schwarz[3]. For this the magnitude of the triplet of the CH_2 group neighbouring the aromatic core of the monomer is compared to the signal of the acetic acid anion after saponification with $NaOD/D_2O$. When evaluating the magnitude of the latter signal, a small triplet resulting from partial H–D exchange on the acetic acid has to be taken into account. By this method the number average *DP* could be obtained within 10% error for smaller molecular weights; higher *DP*s are determined with less accuracy. For PAOB-16 the *DP* thus measured compares favourably with data derived from v.p.o. The *DP*s given by the latter method are in general higher by 10–15% which certainly can be assigned to association in solution. Therefore only *DP*s derived from end-group analysis are used in this work (cf. *Table 3*).

It has been observed that substitution of the poly(4-oxybenzoate) backbone may lower the thermal stability of the resulting polymers considerably[14]. Thermogravimetric measurements on the PAOB-*n* conducted in nitrogen (10 K min^{-1} heating rate) showed these polymers to be stable up to ~350°C. A residual weight loss at lower temperatures can be traced back to the onset of further polycondensation. Nevertheless the oxidative degradation of the side chains represents a severe constraint for the stability at elevated temperatures in the presence of oxygen. All thermogravimetric data obtained so far indicate the upper limit for long-term stability in air to be at temperatures between 160°C and 220°C. Polyesters having longer side chains are more susceptible to degradation. Hence, measurements at elevated temperatures have to be conducted in an inert atmosphere or *in vacuo*.

Another point of great interest is the stiffness of the main chain. Since the unsubstituted polyester is not soluble in any known solvent there are no experimental data on its persistence length. Calculations by Erman *et al.*[15] using the rotational isomeric state model lead to the prediction of a rather rigid chain with a persistence

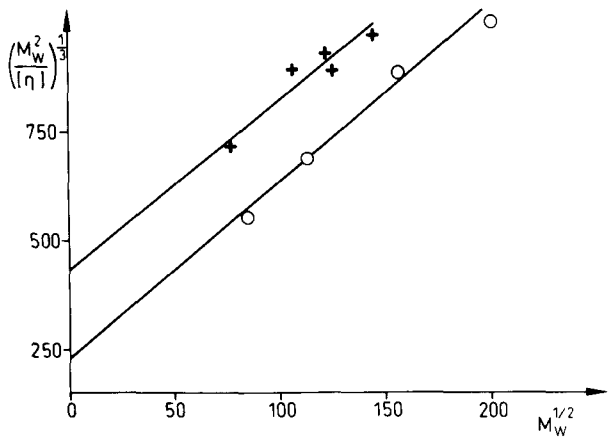

Figure 1 Bohdanecky plot of the intrinsic viscosities of PAOB-3 (○) and PAOB-16 (+)

length of the order of 700 Å. However, these authors remark that such a high value has to be regarded as an upper limit since torsional fluctuation about the ester bonds should lower it appreciably[16]. Molecular dynamics calculations performed by Jung and Schürmann[17] lead to a much smaller value of the persistence length (~60 Å) for this reason. Experimental data on similar polyamides are of limited use for settling this question since the values for the persistence length of these systems given by various methods are not conclusive[1,18]. By virtue of their improved solubility in aprotic solvents the PAOB-*n* are much better candidates for an experimental test of the above conflicting predictions. In the absence of reliable measurements of the radius of gyration by light scattering data, the intrinsic viscosity $[\eta]$ may serve as a first estimate of the chain stiffness. Thus $[\eta]$ has been measured for PAOB-3 in phenol/*o*-dichlorobenzene and for PAOB-16 in tetrachloroethane/*o*-dichlorobenzene at 50°C (cf. *Table 3*). The dependence on temperature as well as the dependence on concentration is well-behaved for these systems whereas solutions of PAOB-16 in toluene and in chloroform did not lead to reproducible results (see above). The resulting Mark–Houwink relations are ($[\eta]$ in dl g^{-1}):

PAOB-3 $[\eta]=6.95\times10^{-2}M_n^{1.06}$
in phenol/*o*-dichlorobenzene at 50°C

PAOB-16 $[\eta]=2.87\times10^{-2}M_n^{1.16}$
in tetrachloroethane/*o*-dichlorobenzene at 50°C

A quantitative interpretation of the data for $[\eta]$ may be given in terms of the worm-like chain model developed by Yamakawa and Fujii[19]. Based on this theory, Bohdanecky[20] has recently given a simple procedure for data evaluation leading to the following relation:

$$(M^2/[\eta])^{1/3}=A_\eta+B_\eta M^{1/2}$$

where A_η is a quantity depending on the hydrodynamic diameter d of the chain and B_η is expressed by

$$B_\eta=B_0\Phi_{0,\infty}^{-1/3}(\langle r^2\rangle_0/M)_\infty^{-1/2}$$

where $\langle r^2\rangle_0$ is the mean-square end-to-end distance, and the subscript ∞ indicates that the $\langle r^2\rangle/M$ value obtained from B_η is the random coil value.

The quantity $\Phi_{0,\infty}$ is the viscosity function for infinite chain length ($\Phi_{0,\infty}=2.86\times10^{23}$)[20]. The quantity B_0 varies between 1.10 and 1.00 and may be set to a mean value of 1.05 at the present level of accuracy. *Figure 1* shows a Bohdanecky plot of the present data. The weight average molecular weights have been calculated from the data given in *Table 3* by assuming a most probable distribution.

The Kuhn length is calculated as $l_K=\langle r^2\rangle/Nl_u$ where $N=M/M_u$ with M_u and l_u being the mass per unit length and the length of the monomer unit, respectively. The latter quantity is given by 6.2 Å in good approximation (see below). From these data and the slope of the respective curves in *Figure 1*, l_K is ~90 Å for PAOB-3 and ~190 Å for PAOB-16. The intercept A_η may be used to yield first estimates of the hydrodynamic radius r according to[20]:

$$\frac{d_r^2}{A_0}=(4\Phi_{0,\infty}1.215\pi N_A)(\bar{v}/A_\eta)B_\eta^4$$

where $d_r=d/l_K$ is the reduced hydrodynamic radius and d_r^2/A_0 is related to d_r by[20]

$$\ln(d_r^2/A_0)=0.173+2.158\ln(d_r)$$

If the partial specific volume $\bar{v}$ of the polymer in solution is approximated by unity, we obtain for PAOB-3 a value in the range 7–8 Å, and for PAOB-16 11–13 Å. Similar values have been found recently for substituted cellulose polymers[21] and seem to be quite reasonable. One has to bear in mind that these values have been derived under a number of stringent assumptions[19,20]. On the molecular level the polymer chain is approximated by a cylinder which may be rather questionable when looking at the structure of PAOB-*n* with $n>6$. Hence, these data should be only regarded as rough estimates and the present investigation of chain stiffness must be certainly supplemented by other methods.

Despite these problems it is clear that our findings data are more in support of the prediction of Jung and Schürmann[17]. Krigbaum and Tanaka[22] recently found l_K values of similar magnitude for poly(phenyl *p*-phenyleneterephthalate) by a variety of methods. Thus the present data indicate that the stiffness of the fully aromatic polyester chain is significantly smaller than anticipated by the calculations neglecting the effect of bond-angle fluctuations. The surprising fact that the stiffness seems to increase with increasing length of the side chains may be explained[23] by the notion that steric interactions between bulky side chains lead to a significant rise in l_K. In the absence of further information on the shape of the PAOB-*n* chain as revealed by small angle X-ray or neutron scattering no firm conclusions can be drawn.

Phase behaviour of PAOB-3

In the following it will become obvious that the phase behaviour of PAOB-3 is significantly different from the phase behaviour of PAOB-*n* bearing longer side chains. In the case of PAOB-3 the main chains control the structure and thermal transitions. For longer side chains the volume fraction of the main chains is decreasing and the most favourable arrangement of the side chains determines the packing of the polymer in the solid state as well as in the mesophase.

Solid state. Figure 2 shows the WAXS patterns of PAOB-3 recrystallized from the melt (*Figure 2a*) and from dioxane (*Figure 2b*). From this it is evident that two different modifications have been formed through

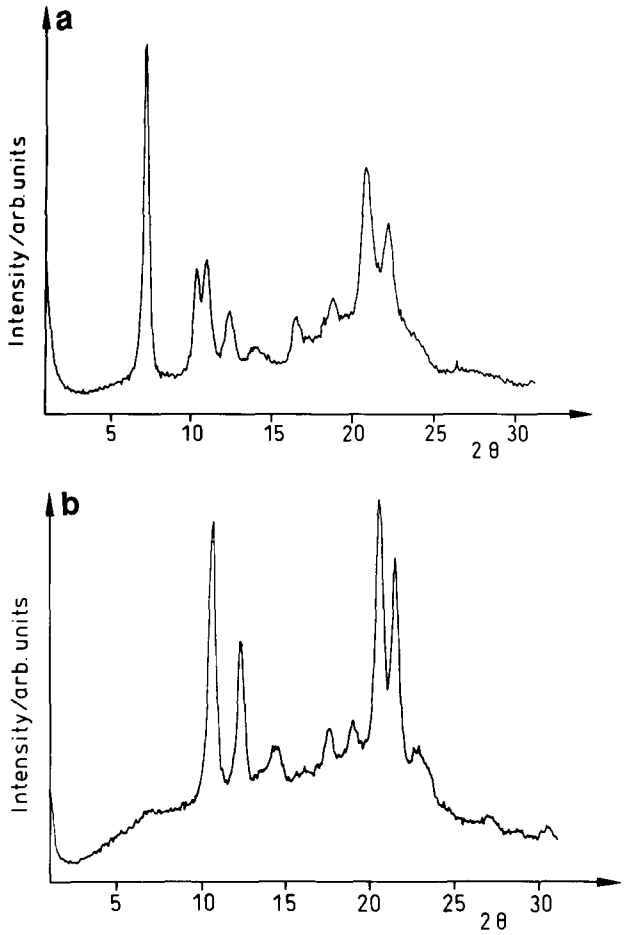

Figure 2 Wide-angle X-ray diffractograms (uncorrected) of PAOB-3 recrystallized from the melt (a) and from dioxane (b)

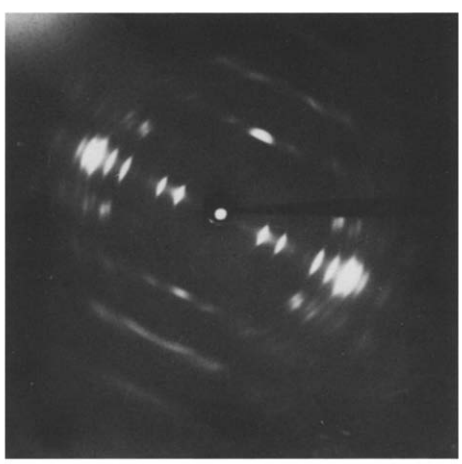

Figure 3 X-ray fibre diagram of PAOB-3 drawn from the melt (modifications Ia and Ib). The Miller indices are given in *Table 4*

the different conditions of crystallization. The WAXS patterns furthermore show both modifications to have a high degree of crystallinity. Melt-crystallized samples (referred to as modification I fibres) with a high degree of orientation may be drawn. The resulting fibre diagram is shown in *Figure 3*.

The distance between the layer lines demonstrates that the identity period along the chain consists of two oxybenzoate monomer units. This is in accordance with the crystal structure of the dimeric model compound[8] in which the planes of subsequent benzene rings are rotated through an angle of 90° with respect to each other. The absence of meridional reflections with odd 1 indices indicates a 2_1 or a 4_2 helical structure of the main chain. An additional feature is the presence of two series of reflections on the different layer lines leading to two hyperbolas per layer. This can be seen most clearly from the splitting of the 0 0 2 reflection. Variations of the *c*-parameter within a range of 12.4–12.9 Å were observed in earlier work on poly(4-hydroxybenzoic acid) and were shown to be a function of the *DP*[5]. All reflections found in this work may be indexed satisfactorily in terms of two tetragonal modifications, Ia and Ib, which differ only with regard to the *c* vector of the unit cell. *Table 4* gives the Bragg distances and their respective indices.

The presence of two very similar modifications Ia and

Table 4 Calculated and observed X-ray reflections of modifications Ia, Ib and II of PAOB-3

Reflection index (*h k l*)	Calculated spacing (Å)	Observed spacing (Å)	Position/modification
Tetragonal modifications Ia and Ib, $a=b=16.95$ Å, $c=12.36$ Å (Ia), $c=12.86$ Å (Ib)			
1 1 0	11.99	11.99(vs)	
0 2 0	8.48	8.47(vs)	
		7.16(vw)	
2 2 0	5.99	5.96(vw)	
1 3 0	5.36	5.34(s)	Equator (*a*, *b*)
2 3 0	4.70	4.70(s)	
0 4 0	4.24	4.24(vs)	
1 4 0	4.11	4.12(m)	
3 3 0	4.00	3.99(s)	
2 4 0	3.79	3.78(m)	
1 5 0	3.32	3.34(w)	
1 2 1	6.46	6.50(vw)	
1 3 1	4.92	4.86(m)	1st layer line: *a*
2 3 1	4.39	4.28(m)	
0 3 1	5.17	5.11(m)	
2 3 1	4.42	4.50(m)	
0 4 1	4.02	4.03(vw)	1st layer line: *b*
2 4 1	3.64	3.68(w)	
1 5 1	3.22	3.19(vw)	
0 0 2	6.18	6.18(s)	
0 1 2	5.81	5.85(w)	2nd layer line: *a*
1 2 2	4.79	4.69(w)	
1 3 2	4.05	3.95(vw)	
0 0 2	6.43	6.43(s)	
0 3 2	5.12	5.08(vw)	2nd layer line: *b*
2 2 2	4.38	4.50(vw)	
0 1 3(*a*)	4.0(*a*)	4.06(m)	
0 1 3/1 1 3(*b*)	4.16/4.04(*b*)		
0 2 3(*a*)	3.71(*a*)	3.77(m)	3rd layer line
0 2 3/1 2 3(*b*)	3.83/3.73(*b*)		
0 0 4	3.09(*a*)	3.11(w)	4th layer line
	3.22(*b*)		

Reflection index (*h k l*)	Calculated spacing (Å)	Observed spacing (Å)	
		X-ray	Electron diffraction
Orthorhombic modification II $a=14.20$ Å, $b=9.60$ Å, $c=12.48$ Å			
1 1 0	7.95	7.94(s)	7.99(s)
2 0 0	7.10	7.07(m)	7.12(s)
0 0 2	6.24	6.24(w)	
0 2 0	4.80	4.72(w[a])	4.83(w)
3 1 0	4.25	4.22(s)	4.25(s)
2 2 0	3.98	3.96(s)	4.00(s)
4 2 0	2.85		2.87(w)

[a] Shoulder of 3 1 0 reflection

Abbreviations: vs, very strong; s, strong; m, medium; w, weak; vw, very weak

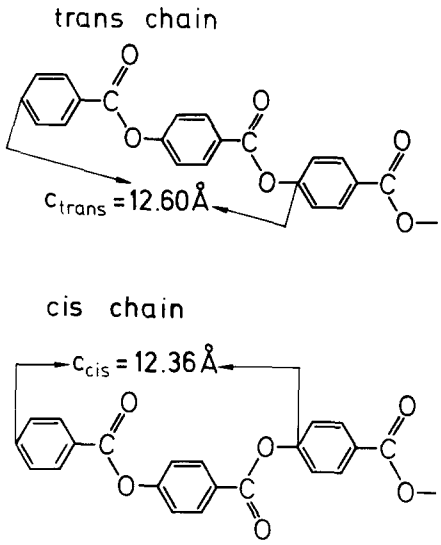

Figure 4 Representation of the *trans* and *cis* conformers of the *p*-oxybenzoate backbone together with the calculated *c* values (modifications Ia and Ib)

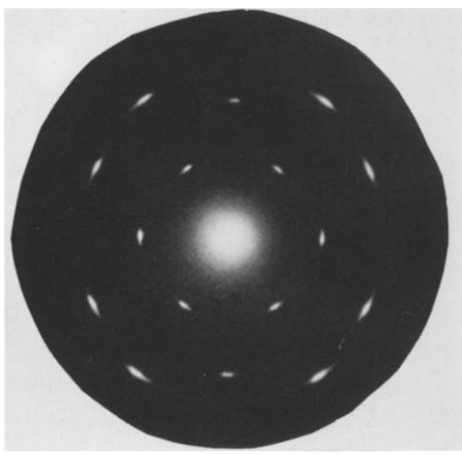

Figure 5 Electron diffraction of PAOB-3 recrystallized from dioxane (modification II). *Table 4* gives the Miller indices

Ib may be due to the formation of crystals with different conformation of the main chains (*Figure 4*). The length of the identity period along the *c* direction can be calculated from the bond lengths and angles derived from the crystal structure of the dimer. This leads to 12.60 or 12.36 Å for the *trans* and *cis* chains, respectively. The values derived from the analysis of the fibre diagram (Ia: 12.36; Ib: 12.86) compare favourably with these deductions if the slightly higher value of *c* found for Ib is explained in terms of small distortions of bond angles. Also the mean value of the theoretical density (1.190 g cm^{-3}) is in accordance with the experimental result (1.183 g cm^{-3}). The only reflection not being indexed by the above unit cell corresponds to a Bragg distance of 7.16 Å and is the strongest one of a series of reflections (21.3, 10.7, 7.1). The most probable explanation for this is the assumption of a third orthorhombic modification Ic which seems to be formed during solid state polycondensation (cf. ref. 4 for similar observations on the unsubstituted polyester).

In the case of solution-crystallized samples (cf. *Figure 2b*) the corresponding structure may be elucidated by electron diffraction applied to small crystallites formed by material with lower degrees of polymerization. Since crystallites of stiff polymers usually have dimensions which are much larger in the direction perpendicular rather than parallel to the chains[4], these crystallites will lie flat on the 0 0 1 surface. Thus with this geometry (electron beam perpendicular on the crystal surface) only *h k* 0 reflections will be monitored. *Figure 5* shows the result whereas *Table 4* gives the *d*-spacings of modification II which can be indexed by an orthorhombic unit cell ($a = 14.20$ Å, $b = 9.60$ Å, $c = 12.48$ Å, four chains per unit cell). The 6.24 Å reflex which is only visible in the WAXS diffractogram (*Figure 2b*) is interpreted as the 0 0 2 reflex in analogy to modification I. The length of the repeating unit (12.48 Å) is the mean value of the data derived from the *cis* and *trans* chains (see above). The X-ray density (1.27 g cm^{-3}) is similar to values (1.2–1.3 g cm^{-3}) found for the solution-crystallized oligomers[8].

Elevated temperatures. All PAOB-3 samples exhibit a broad bimodal melting peak with temperatures depending on molecular weight. Since the specimens having a smaller *DP* still contain reactive end groups, heating up leads to further polycondensation. Second runs in consequence exhibit higher melting temperatures. If the materials are annealed at the temperature of the lower melting peak a second run only gives a single sharp melting transition at $T = 294$°C and no indication of a glass transition (*Figure 6*).

This value nearly coincides with the melting point of the oligomers extrapolated to infinite molecular weight[8]. It is thus concluded that the crystallinity in the annealed material is very high. This finding is already obvious from the fibre diagrams of melt-drawn specimens. In this context it is interesting to note that the heat of fusion (36 J g^{-1}) is approximately equal to the value found[3] for the high temperature solid–solid transition (38 J g^{-1}) of the unsubstituted poly(4-oxybenzoate). WAXS diffractograms and polarizing microscopy however, revealed that PAOB-3 is transformed into an ordinary nematic phase. No transition to the isotropic fluid occurred within the accessible range of temperature. The extrapolation of the transition temperatures obtained from oligomers to infinite molecular weight indicates[8] the T_{ni} of the polymer to be located at ~430°C, i.e. where thermal decomposition prevails.

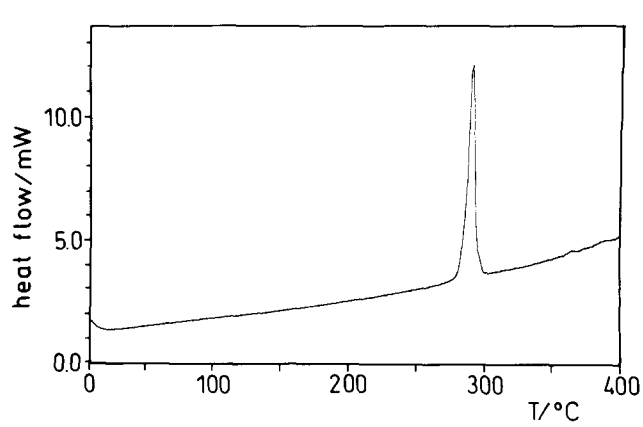

Figure 6 Differential scanning calorimetry analysis of an annealed sample of PAOB-3 at 20 K min^{-1}

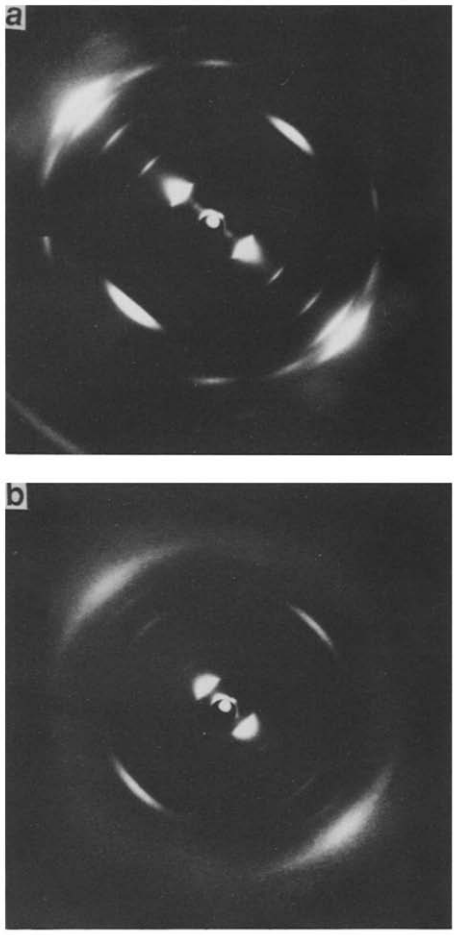

Figure 7 X-ray fibre diagram of PAOB-5 (a) and PAOB-10 (b) monitored at room temperature. The Miller indices (modification III) are given in *Table 5*

Phase behaviour of PAOB-5 to PAOB-18

As shown for PAOB-3, the structure of the polyester strongly depends on the preparation of the sample. The PAOB-*n* having large side chains exhibit the same feature. In the following, three modifications termed III, IV and V are described. Modification III results from melt, IV is prepared through precipitation from solution and V is formed when casting films from solutions in chloroform. As a common feature all three structures are organized in layers, the spacings of which depend on the length of the side chains.

Solid state: modification III. Oriented samples of this modification are obtained by drawing fibres from melt or stretching films at temperatures between 120°C and 170°C. All specimens thus obtained are highly oriented and exhibit an uniaxial texture. The resulting fibre diagram for PAOB-5 is displayed in *Figure 7a*.

The off-meridional reflections point to a well-developed three-dimensional order. Longer side chains are followed by a loss of these long range correlations and only meridional and equatorial reflections remain. *Figure 7b* demonstrates this by displaying the fibre diagram obtained from PAOB-10. The reflections shown in *Figure 7* for PAOB-5 can be indexed in terms of an orthorhombic unit cell with the parameters $a=17.8$ Å, $b=9.6$ Å, $c=12.6$ Å, $d=1.155$ g cm^{-3}, with four chains in the unit cell. The respective indices are given in *Table 5*. Here, as in modifications I and II of PAOB-3, the identity period along the chain consists of two monomer units. However, there is no splitting into *cis* or *trans* segments, the chains seem to contain both forms in statistical sequence. A comparison with modification II of PAOB-3 shows the magnitude of b to be identical. From *Table 5* and *Figure 7b* it is obvious that the gradual loss of long-range correlation does not allow an unambiguous assignment of the unit cell owing to the absence of mixed reflections. On the other hand, all reflections of PAOB-6 can be satisfactorily indexed in terms of modification III (cf. *Table 5*). No new feature appears in the fibre diagrams

Table 5 Calculated and observed X-ray reflections of orthorhombic modification III (PAOB-5 to PAOB-18) $a=\cdots$, $b=9.6$ Å, $c=12.6$ Å

Reflection index ($h\,k\,l$)	Calculated spacing (Å)	Observed spacing (Å)	Position
PAOB-5			
1 0 0	17.80	17.75(vs)	
2 0 0	8.90	8.90(m)	
3 0 0	5.93	5.92(m)	
4 0 0	4.45	4.43(m)	Equator
0 2 0	4.80	4.80(s)	
2 2 0	4.22	4.34(s)	
3 3 0	2.82	2.86(w)	
		4.45(w,d)	
0 2 1/3 1 1	4.5/4.6	4.6(m)	
2 2 1	4.0	4.0(vw)	1st layer line
3 2 1/4 1 1	3.6/3.8	3.7(vw)	
0 0 2	6.3	6.3(s)	
0 1 2/2 0 2	5.3/5.1	5.2(vw)	
2 1 2	4.5	4.7(m)	
3 0 2	4.3	4.3(vw)	2nd layer line
0 2 2/3 1 2	3.8/3.9	3.9(m)	
0 2 2/1 2 2	3.8/3.7	3.7(vw)	
0 0 4	3.15	3.1(m)	4th layer line
4.6 Å (vw,d): halo			
PAOB-6			
1 0 0	19.80	19.80(vs)	
2 0 0	9.90	9.91(vw)	
3 0 0	6.60	6.60(w)	
4 0 0	4.95	4.96(m)	Equator
5 0 0	3.96	4.00(vw)	
		4.47(m,d)	
0 2 1/4 0 1	4.5/4.6	4.60(w)	
2 2 1	4.1	4.00(vw)	1st layer line
0 0 2	6.25	6.25(s)	
1 1 2	5.10	5.00(w)	2nd layer line[a]
0 0 4	3.15	3.10(w)	4th layer line
4.6 Å (w,d): halo			
PAOB-10			
1 0 0	26.80	27.00(vs)	
2 0 0	13.40	13.38(vw)	Equator
4 0 0	6.70	6.70(w)	
5 0 0	5.36	5.37(vw)	
		4.53(m,d)	
		4.50(vw,d)	1st layer line
0 0 2	6.25	6.25(s)	2nd layer line
		4.90(vw,d)	
0 0 4	3.15	3.10(vw)	4th layer line
4.15 Å (w,d): halo			

[a] Calculated under assumption $b=9.6$ Å

PAOB-12 to PAOB-18: only strong 1 0 0 reflection on the equator, higher orders weak or not visible, distinct 0 0 1 (1 even) reflections, halo at 4.5 Å

Abbreviations: vs, very strong; s, strong; m, medium; w, weak; vw, very weak; d, diffuse

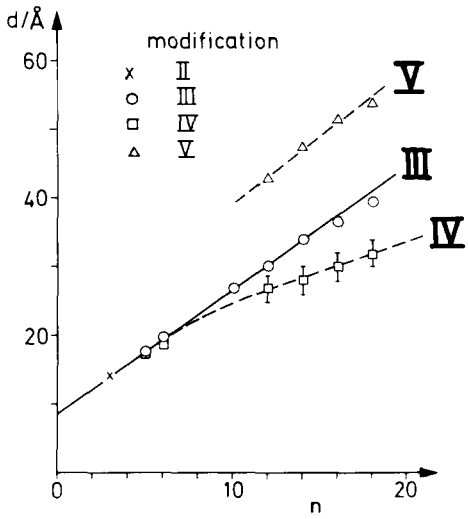

Figure 8 Layer spacings ($h\,0\,0$ reflections) of modifications II–V as a function of the number n of carbon atoms in the side chains

when appending longer side chains. Therefore it seems reasonable to assume a distorted orthorhombic unit cell for PAOB-10 to PAOB-18 too. Thus the layer reflections on the equator visible in all fibre diagrams can be interpreted as the $h\,0\,0$ reflections of modification III; the variation with side chain length n is shown in *Figure 8*. The cross denotes the magnitude of the a vector of the unit cell of modification II (see previous section). The linear dependence of parameter a on n strongly suggests that the side chains extend into the a direction. The increment per CH_2 group is 0.9 Å and the intercept is 8.6 Å. The value of modification II of PAOB-3 (see previous section) fits the corresponding data obtained from modification III very well. This, together with the fact that the b value (seen for PAOB-5) is unaffected by the length of the side chains, indicates that the positions of the side chains are the same for both modifications. The long-range correlation in the b direction which leads to a distance of 4.8 Å between the main chains of PAOB-3 (II) and PAOB-5 (III) is no longer present in PAOB-n with $n \geqslant 6$. There is no 0 2 0 reflection but a halo appears with a maximum at a Bragg distance of 4.5 Å (cf. *Table 5*). From a comparison of the measured and calculated densities the mean distance between the main chains is 4.8–5.0 Å, i.e. a slightly higher value than found for PAOB-5. This is in accordance with the distance calculated by a modified Bragg equation[24]

$$2d \sin \frac{\Theta}{2} = f\lambda$$

from the halo. The above distance of the order of 5 Å requires $f \simeq 1.11$. This agrees with values calculated for systems with similar disorder[24].

All the findings can be put together into a model of the molecular arrangement in modification III (*Figure 9*). From the intercept of 8.6 Å we suggest that two main chains are lying together. The side chains do not intercalate but form a mean angle of 46° with the main chains. This follows directly from a comparison of the maximum increment per CH_2 group (1.25 Å) and the slope (0.9 Å) found in *Figure 8*. The average distance between the side chains in the ac plane is ~4.5 Å which approximately corresponds to the layer spacing in the rotator phase of paraffins[25]. The lack of a reflection

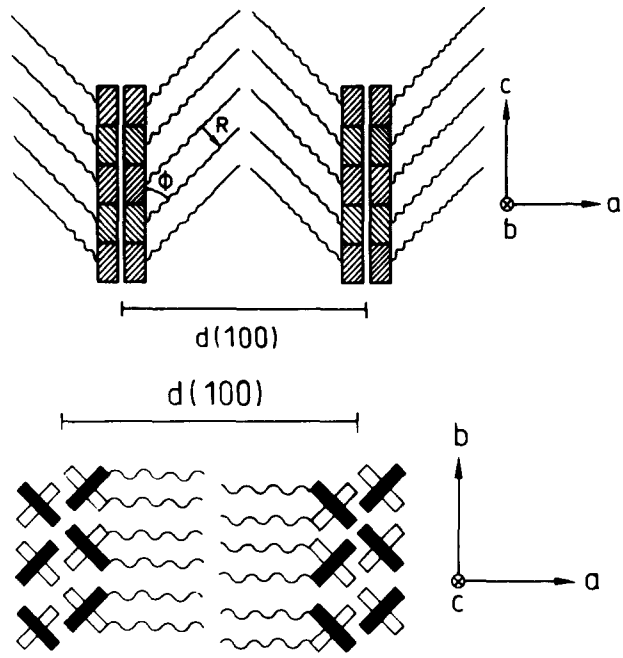

Figure 9 Schematic representation of molecular arrangement of main and side chains in modification III of PAOB-5 to PAOB-18

superposing the broad halo at a Bragg spacing of ~4.5 Å leads to the suggestion that the side chains are packed in a rather disordered fashion. The halo becomes more intense with increasing side chain length indicating that the fraction of disordered alkyl chains becomes increasingly important. Investigations on a number of comb-like polymers have shown that the first 8–10 CH_2 units cannot crystallize[26]. For the PAOB-n under consideration here d.s.c. measurements show that side chain crystallization requires $n \geqslant 12$. This may explain that in the cases of $n = 16$ and 18 the magnitude of a is slightly smaller than the value extrapolated from smaller n (*Figure 8*). The closer packing of the alkyl chains in the crystallites requires a smaller distance and hence a smaller angle with the main chains. The intercept of 8.6 Å which corresponds to the width of the aromatic layer indicates that the benzene rings of neighbouring chains are not face to face but as shown in *Figure 9*. Therefore the angle between subsequent phenyl groups within one chain must be of the order of 90° in agreement with previous deductions[8]. The above model requires that the first 8–10 CH_2 units are packed in a liquid-like disordered fashion, subsequent units are packed in a more regular way. An argument in favour of this conclusion is derived from the calculated density in the alkyl layer: the volume per CH_2 results $\sim 0.9/2 \cdot b/2 \cdot c/2$ where the first factor is the length of one unit in the a direction. Thus $d_{CH_2} = 0.86$ g cm^{-3} which agrees very well with the density derived for amorphous polyethylene (0.855 g cm^{-3})*.

Modification IV. Figure 10 shows a diffractogram obtained from PAOB-18 through precipitation from solutions in chloroform into methanol. In the wide angle region (*Figure 10*) there is only one broad peak with a maximum at ~4.5 Å and a weak reflection at ~6.1–6.2 Å which may be interpreted as a 0 0 2 reflection. The position of a small-angle reflection coincides with the

* Extrapolated value, cf. reference 13

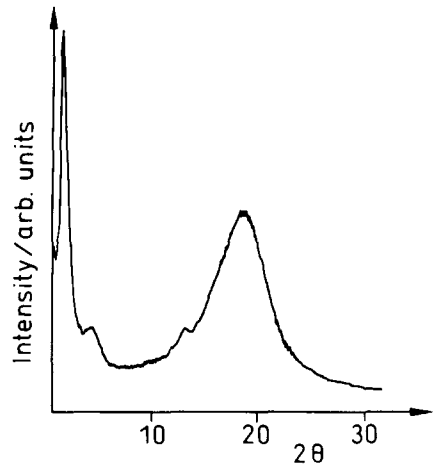

Figure 10 Wide-angle X-ray diffractogram (uncorrected) of PAOB-18 precipitated from solution (modification IV)

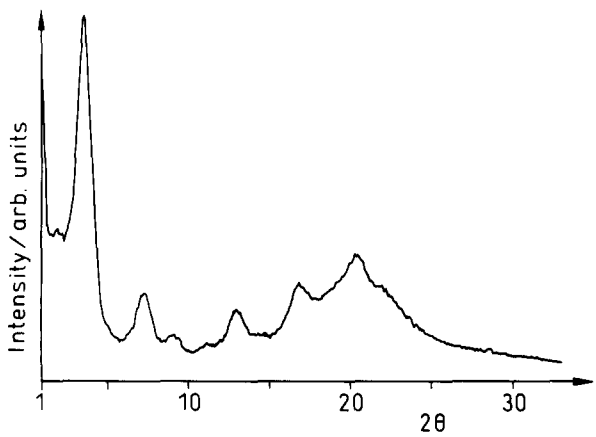

Figure 11 Wide-angle X-ray diffractogram (uncorrected) of a film cast from solutions of PAOB-18 (modification V)

data obtained for III as long as $n<10$ (*Figure 8*) but deviates from the straight line if $n \geqslant 12$ (cf. *Figure 8*). Here the *d*-spacing is not constant for a given *n* but fluctuates for different specimens around a mean value. Thus one has to conclude that up to $n=10$ the specimens obtained by precipitation crystallize in modification III, beyond this point the considerably smaller *d*-spacing indicates much denser packing of the side chains as compared to the arrangement in the melt crystallized samples. This conjecture finds support from thermal analysis (see below). The dependence of the spacing on the history of the sample however, questions whether modification IV can be regarded as an equilibrium state.

Modification V. A third modification for PAOB-*n* with $n \geqslant 12$ is obtained by casting films from solution. The broad reflections visible in the WAXS diffractogram (*Figure 11*) can be indexed by a layered structure. In all cases the first order could not be measured by the wide angle diffractometer but had to be inferred from the higher orders ($n=12$, 42.9 Å; $n=14$, 47.4 Å; $n=16$, 51.4 Å; $n=18$, 54.0 Å). X-ray photographs with the beam parallel and perpendicular to the surface of the film revealed the layers to be oriented preferentially parallel to the surface. Heating up to temperatures of the mesophase, however, lead to a loss of this orientation. Therefore no oriented fibres could be analysed. As a consequence the present data do not allow detailed conclusions of the structure of modification V. The width of the WAXS peaks indicates that the layered structure is strongly distorted.

Phase behaviour at elevated temperatures

The polyesters having intermediate length ($5 \leqslant n \leqslant 10$) side chains behave in a rather similar fashion as observed for PAOB-3. The occurrence of two glassy transitions is interesting to note (PAOB-5: $T_{g1} \simeq 50°C$, $T_{g2} \simeq 140°C$). Also the rather broad melting peak is considerably sharpened when annealing the materials closely below the peak maximum. For longer side chains additional transitions appear in the region $-30°C$ to $100°C$ depending on the respective modification. This can be seen by comparing the thermograms of PAOB-18 obtained by precipitation from solution (*Figure 12a*, modification IV) and by casting films from chloroform (*Figure 12b*, modification V).

In analogy to a great number of comb-like polymers[26] the low temperature transition is assigned to a 'melting' process of the side chains. Depending on the order in the alkyl layers the temperature of this transition is shifted to higher temperatures. From *Figure 12* it is also evident that there is always a mixture of different modes of side chain crystallization. Modification V is obviously characterized by a more regular packing. Annealing leads to a variation of the contents of more or less ordered side chains. The present experimental observations are not yet sufficient for more detailed conclusions regarding the arrangement and the order of the side chains.

All PAOB-*n* form mesophases at elevated temperatures. This could be clearly demonstrated by polarizing microscopy. All mesophases turned isotropic at the

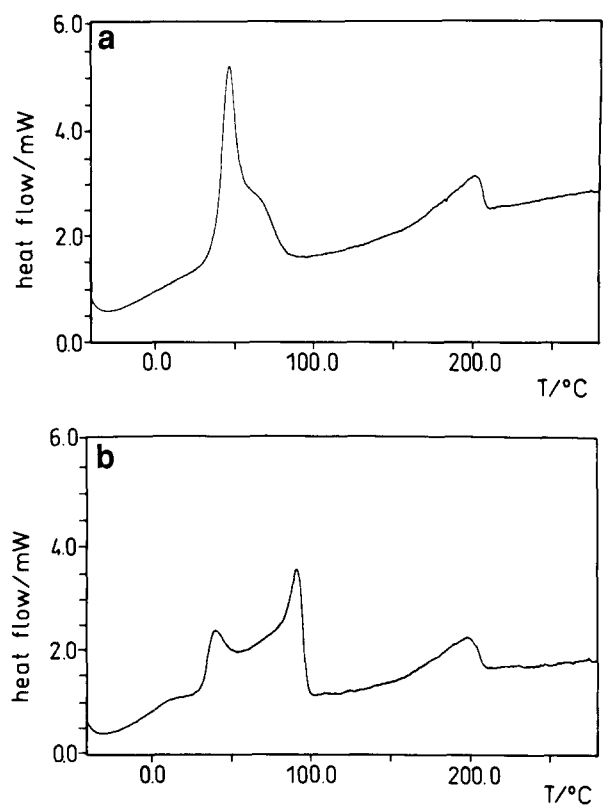

Figure 12 Differential scanning calorimetry thermogram (20 K min^{-1}) of PAOB-18 precipitated from solution (a, modification IV) and of PAOB-18 films cast from solution (b, modification V)

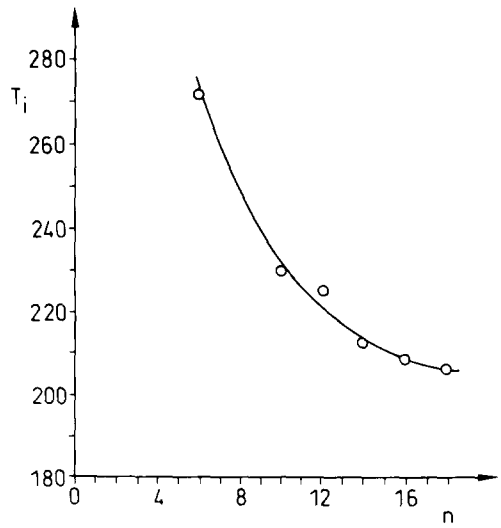

Figure 13 Isotropization temperatures of PAOB-5 to PAOB-18 as a function of n the number of carbon atoms in the side chains

temperature displayed in *Figure 13*. The data shown in *Figure 13* have to be compared cautiously because of their dependence on molecular weight. However, the lowering of the clearing point by an increasing number of carbon atoms in the side chains is clearly visible. Cooling down again leads to the formation of the mesophase but with considerable supercooling. Polarizing microscopy did not give conclusive information on the nature of the mesophase. The WAXS diffractograms unambiguously demonstrated that PAOB-n with $n \geqslant 6$ form layered mesophases. This is directly seen from the sharp layer reflection (*Figure 14*) together with the halo in the wide-angle region indicating a liquid-like short-range order. Unoriented nematic or isotropic phases only exhibit a weak halo in the small-angle region where the sharp Bragg reflection appears. For PAOB-5 the layered mesophase seen after melting the crystalline modification III transforms first into a nematic phase at 275°C which turns isotropic at 345°C. Thus this polymer represents an intermediate between the PAOB-3 forming only nematic phases and the PAOB-n with $n \geqslant 6$ forming only layered mesophases. A similar transition from a layered mesophase to a nematic phase has been observed for the poly(2,5-dihexoxy-1,4-phenyleneterephthalate)[27].

CONCLUSIONS

Appending of n-alkyl side chains to the p-oxybenzoate backbone leads to soluble polyesters whereas the unsubstituted poly(p-oxybenzoate) does not dissolve in any known solvent[3]. The sufficient solubility allows the estimation of l_K from viscosity data. The resulting l_K is of the order of 100–200 Å and increases with increasing length of the side chains. The unit cells of the room temperature modifications I–III could be determined. Short side chains are packed into these units cells (modifications Ia, Ib, II) in an ordered fashion leading to a high degree of crystallinity. Longer side chains are followed by an increasing disorder and the loss of correlation between the chains (see the discussion of modification III). All PAOB-n form thermotropic mesophases with liquid-like short-range order whereas the unsubstituted poly(4-oxybenzoate) is transferred to a pseudohexagonal high-temperature modification[5]. If $n = 3$,

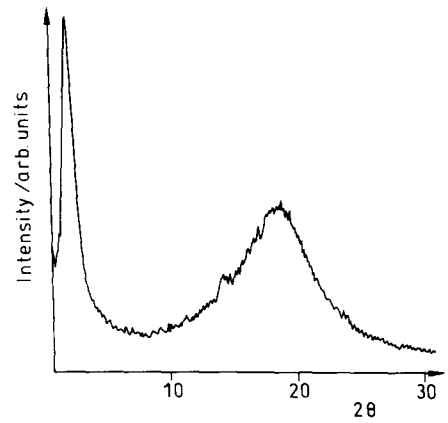

Figure 14 Wide-angle X-ray diffractogram (uncorrected) of PAOB-16 monitored at 150°C

the mesophase is nematic, PAOB-5 exhibits a transition from a layered mesophase to the nematic state and finally to an isotropic phase. If $n > 5$, solely layered smectic-like mesophases are observed. Thus the PAOB-n has a phase behaviour as observed recently for a number of similar systems[1].

ACKNOWLEDGEMENTS

Financial support of the Bundesminister für Forschung und Technologie, Projekt 'Steife Makromoleküle', is gratefully acknowledged. The authors are indebted to M. Schmidt for helpful discussions.

REFERENCES

1 Ballauff, M. *Angew. Chem.* 1989, **101**, 261; *Angew. Chem. Int. Edn.* 1989, **28**, 253
2 Economy, J., Storm, R. S., Matkovich, V. I. and Cottis, S. G. *J. Polym. Sci., Polym. Chem. Edn.* 1976, **14**, 2207
3 Kricheldorf, H. R. and Schwarz, G. *Makromol. Chem.* 1983, **184**, 475
4 Lieser, G., Schwarz, G. and Kricheldorf, H. R. *J. Polym. Sci., Polym. Phys. Edn.* 1983, **21**, 1599
5 Lieser, G. *J. Polym. Sci., Polym. Phys. Edn.* 1983, **21**, 1611
6 Hanna, S. and Windle, A. H. *Polymer* 1988, **29**, 236
7 Economy, J., Volksen, W., Viney, C., Geiss, R., Siemens, R. and Karis, T. *Macromolecules* 1988, **21**, 2777
8 Stern, R., Enkelmann, V. and Wegner, G. in preparation
9 Claisen, L. and Eisleb, O. *Liebigs Ann. Chem.* 1913, **401**, 85
10 Cox, E. H. *J. Am. Chem. Soc.* 1930, **52**, 352; Blatt, A. H. *Org. React.* 1942, **1**, 342
11 Organikum, VEB Deutscher Verlag der Wissenschaften, Berlin, 1971
12 Hartung, W. H. and Simonoff, R. *Org. React.* 1953, **7**, 263; Read, R. R. and Wood, J. *Org. Synth. Coll. Vol.* 1955, **3**, 444
13 Hoffmann, M., Krömer, H. and Kuhn, R. 'Polymeranalytik', Thieme-Verlag, Stuttgart, 1977
14 Kricheldorf, H. R. and Schwarz, G. *Polymer* 1984, **25**, 520
15 Erman, B., Flory, P. J. and Hummel, J. P. *Macromolecules* 1980, **13**, 484
16 Birshtein, T. M. *Polym. Sci. USSR* 1977, **19**, 60
17 Jung, B. and Schürmann, B. L. *Macromolecules* 1989, **22**, 477
18 Zero, K. and Aharoni, S. M. *Macromolecules* 1987, **20**, 1957
19 Yamakawa, H. and Fujii, M. *Macromolecules* 1974, **7**, 128
20 Bohdanecky, M. *Macromolecules* 1983, **16**, 1483
21 Mays, J. W. *Macromolecules* 1988, **21**, 3179
22 Krigbaum, W. R. and Tanaka, T. *Macromolecules* 1988, **21**, 743
23 Aime, J.-P. and Bargain, E. *Europhys. Lett.* 1989, **9**, 35
24 Alexander, L. A. 'X-Ray Diffraction Methods in Polymer Science', Krieger, Huntington, NY, 1979
25 Müller, A. *Proc. R. Soc.* 1932, **A138**, 514
26 Platé, N. and Shibae, V. P. 'Comb-Shaped Polymers and Liquid Crystals', Plenum, New York, 1987
27 Falk, K. and Spiess, H. W. *Makromol. Chem. Rapid Commun.* 1989, **10**, 149